CONVERGENCE ANALYSIS OF ACTIVE CONTOURS IN IMAGE SEGMENTATION

Rafael Verdú, Juan Morales, Ricardo González

* Universidad Politécnica de Cartagena
Muralla del Mar s/n, 30202, Cartagena, Spain
rafael.verdu@upct.es

Luis Weruaga

Austrian Academy of Sciences
Donau-City Strasse 1, 1220 Vienna, Austria
weruaga@ieee.org

ABSTRACT

Active contours effectiveness in image segmentation is well known. As any adaptive system, the iterations required by the contour to delineate the target is of importance. In this process, some nodes reach their position before than others, and, due to the internal forces, the neighboring nodes evolve towards a final shape constrained to the external forces. This paper presents a signal-processing perspective of that scenario by deriving a novel frequency-based formulation. The main result of the analysis is the speed of convergence, which depends analytically on the stiffness properties, and especially on the second-order parameters and the length of the snake segments. This initial attempt to characterize the snake dynamics is supported with simulation results.

1. INTRODUCTION

Active contours or snakes have been widely used in image processing and computer vision, as a smart technique for image segmentation, for tracking moving objects in video, and to interpolate noisy image and corrupted data. The basic principle behind is the ability to draw a smooth parametric curve constrained to external requirements, in an adaptive way by means of an iterative mechanism.

Apart from its original Lagrangian formulation [1], several types and variants of active deformable models have been since then proposed [2], but the parametric characteristics of the first one offer important advantages in several problems, especially in interpolation and segmentation of scattered fuzzy data [3][4]. Given the iterative nature of the snake mechanism, knowledge of the speed of convergence to the final situation is desirable. This is important not only when using a regular snake, but especially when combining the basic snake mechanism with another adaptive algorithm with the aim to control certain features of the snake [4]: there a good knowledge of the snake convergence is a must for preventing from an unstable behavior. However an analysis of the transient state has not been done yet.

*This work is partially supported by *Ministerio de Ciencia y Tecnología*, under grant TIC2002-03033.

A novel frequency-based formulation of active contours is being currently proposed [5]: the Lagrangian is solved in the frequency domain, giving rise to an easy design procedure and a economic implementation. Supported on this frequency-based formulation, an analysis of the convergence of active contours is presented in this paper. The scenario to carry out the analysis is the problem of image segmentation, understood as the process in which some nodes are attracted first by external forces, and the minimization of the energy functional makes the contour move to a equilibrium state. The analysis and results in the paper represent our initial work on determining the dynamics and convergence of the snakes, required for further control algorithms.

2. CONVERGENCE ANALYSIS OF SNAKES

A parametric active contour is a time-varying curve $v(s,t)$ whose shape is governed by an energy functional of internal and external forces, $E(\mathbf{v}) = S(\mathbf{v}) + P(\mathbf{v})$ [6]. The internal deformation energy is defined as

$$S(\mathbf{v}) = \int_0^L \alpha(s) \left|\frac{\partial \mathbf{v}}{\partial s}\right|^2 + \beta(s) \left|\frac{\partial^2 \mathbf{v}}{\partial s^2}\right| \, ds, \tag{1}$$

with α and β being the so-called elasticity and rigidity parameters, and s the space index. The external forces $P(\mathbf{v})$ depend on the values of the snake as input to an external function. For a practical implementation, the snake is divided in sub-elements. Collecting the node values of all elements into the vector $\mathbf{u} = [u_1, u_2, ...u_n]$ yields to the discrete-space discrete-time equations of motion [6],

$$\mathbf{A}\,\mathbf{u}_\xi = \mathbf{b}\,\mathbf{u}_{\xi-1} + \mathbf{c}\,\mathbf{u}_{\xi-2} + \mathbf{g}_\xi, \tag{2}$$

where ξ is discrete-time, $\mathbf{b} = 2\mathbf{M} + \mathbf{C}$, $\mathbf{c} = -\mathbf{M}$, $\mathbf{A} = \mathbf{M} + \mathbf{C} + \mathbf{K}$, $\mathbf{M}$ and $\mathbf{C}$ are the mass and damping (diagonal) matrices respectively, $\mathbf{K}$ is the stiffness matrix, and $\mathbf{g}$ is the external force vector. The stiffness matrix $\mathbf{K}$ is a banded matrix (few elements around the diagonal are non-zero), it is assembled from the stiffness submatrices of all elements, and set the relationship among neighboring nodes.

2.1. Defining the application scenario

In spite of the spatial-variant nature of the elements in (2), the work in [5] contains a proof of the equivalence of (2) as a spatial-invariant filtering[1]. Then, the energy functional lies on the stiffness kernel $k(n)$, whose Fourier transform is

$$K(\omega) = \alpha \left|1 - e^{-j\omega}\right|^2 + \beta \left|1 - e^{-j\omega}\right|^4, \tag{3}$$

where ω is frequency, and (2) can be written as

$$\eta^{-1}(\eta + k[n]) * u_\xi[n] = b\, u_{\xi-1}[n] + c\, u_{\xi-2}[n] + x_\xi[n], \tag{4}$$

where $\eta = M + C$ is the global mass, $b = 1 + (1+\gamma)^{-1}$ and $c = -(1+\gamma)^{-1}$ are the second-order parameters, $\gamma = C/M$ is the damping-mass ratio, n is the discrete-space (also the node index), $*$ denotes convolution, $u_\xi[n]$ and $x_\xi[n]$ are respectively the signals that contain the node values and the external forces applied on them at iteration ξ.

In a classical problem of segmentation with active contours, at a certain point of the process some snake nodes, non-uniformly spaced, are "attached" to some high energy regions, and the rest of the nodes are free (see Fig. 1 for a graphical explanation). This scenario can be expressed as a non-uniform interpolation problem by reshaping (4) into

$$z_\xi[n] = b\, u_{\xi-1}[n] + c\, u_{\xi-2}[n], \tag{5}$$

$$y_\xi[n] = z_\xi[n] + (x_\xi[n] - z_\xi[n]) \sum_{k=-\infty}^{\infty} \delta[n - N_k], \tag{6}$$

$$u_\xi[n] = h[n] * y_\xi[n], \tag{7}$$

where N_k are the positions of the nodes attracted by the external forces, and $h[n]$ is the pseudo-inverse kernel of $k[n]$, i.e., its Fourier transform is

$$H(\omega) = \frac{\eta}{\eta + K(\omega)}, \tag{8}$$

Note that (6) is a direct replacement of the node value.

In the next section the case of the external forces being uniformly-spaced, that is, $N_k = k\,N$ is analysed. Its extension to the general non uniformly-spaced situation is considered afterwards.

2.2. Translation to the frequency domain

Equations (5)-(7) can be translated into the frequency domain, resulting

$$Z_\xi(\omega) = b\, U_{\xi-1}(\omega) + c\, U_{\xi-2}(\omega), \tag{9}$$

$$Y_\xi(\omega) = Z_\xi(\omega) - \frac{1}{N} \sum_{k=0}^{N-1} Z_\xi(\omega - k\omega_0) + X_\xi(\omega), \tag{10}$$

$$U_\xi(\omega) = H(\omega) Y_\xi(\omega), \tag{11}$$

[1]Note that in the common case of mass, damping and stiffness being node-independent, the proof of that equivalence is straightforward.

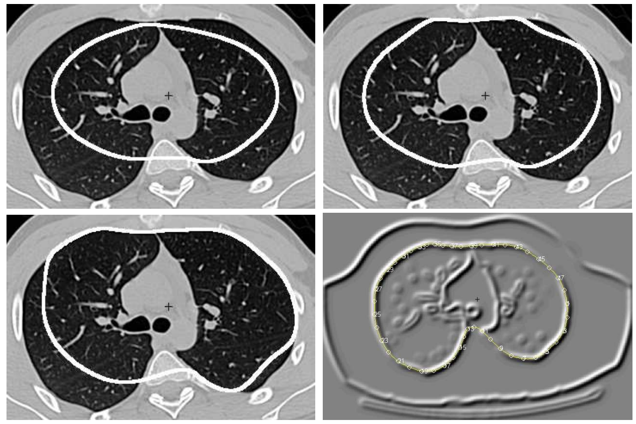

Fig. 1. Sequence of the lung-thorax segmentation by means of a closed snake, and image of external forces (laplacian).

where $\omega_0 = 2\pi/N$. Given that $X_\xi(\omega) = X_\xi(\omega - k\omega_0)$, and by assuming initial repose, then $U_\xi(\omega) = G_\xi(\omega) X_\xi(\omega)$, equations (9)-(11) result in

$$\begin{aligned} G_\xi(\omega) = {} & b\, H(\omega) G_{\xi-1}(\omega) + c\, H(\omega) G_{\xi-2}(\omega) \\ & - b\, H(\omega) \frac{1}{N} \sum_{k=0}^{N-1} G_{\xi-1}(\omega - k\,\omega_0) \\ & - c\, H(\omega) \frac{1}{N} \sum_{k=0}^{N-1} G_{\xi-2}(\omega - k\,\omega_0) + H(\omega). \end{aligned} \tag{12}$$

Equation (12) shows that for a given ω, the equivalent filter $G_\xi(\omega)$ depends on the values of this at frequencies equal to $\omega + k\omega_0$. By considering frequencies $\omega = i\omega_0 + \Delta\omega$ ($i = 0, ..., N-1$, and $|\Delta\omega| \le \omega_0/2$), (12) yields to

$$\mathbf{g}_\xi = \mathbf{h} + \mathbf{H}\,(b\,\mathbf{g}_{\xi-1} + c\,\mathbf{g}_{\xi-2}), \tag{13}$$

where $\mathbf{g}_\xi = [G_\xi(\Delta\omega),\, G_\xi(\omega_0 + \Delta\omega),\, \ldots,\, G_\xi((N-1)\omega_0 + \Delta\omega)]^T$, $\mathbf{h}$ defined accordingly, and matrix $\mathbf{H}$ is

$$\mathbf{H} = \mathrm{diag}(\mathbf{h}) - \frac{1}{N}\,\mathbf{h}\,[1 \overset{N}{\cdots} 1]. \tag{14}$$

In the steady state ($\xi = \infty$), (13) leads to

$$\mathbf{g} = (\mathbf{I} - \mathbf{H})^{-1}\,\mathbf{h}. \tag{15}$$

The equivalent kernel in the steady state is described by (15). The inverse process, that is, drawing kernel $H(\omega)$ from a desired final situation $G(\omega)$ has no easy explicit formulation. Generally speaking, $G(\omega)$ depends on the stiffness parameters, and on the overall mass η (8). This means that for constant η, the solution reached in the steady state is the same regardless of the ratio damping-mass γ. However, the speed of the snake towards that final situation does depend on γ, as shown in the next section.

2.3. Analysis of convergence

Subtraction of the final value in the recursion (13), that is, $\mathbf{r}_\xi = \mathbf{g}_\xi - \mathbf{g}_\infty$, gives rise to the linear difference equation that describes the residual evolution of the active contour

$$\mathbf{r}_\xi = b\,\mathbf{H}\,\mathbf{r}_{\xi-1} + c\,\mathbf{H}\,\mathbf{r}_{\xi-2}. \tag{16}$$

Matrix $\mathbf{H}$ can be expressed as $\mathbf{H} = \mathbf{LDL^{-1}}$, $\mathbf{D}$ being a diagonal matrix of eigenvalues $\lambda_1, ..., \lambda_N$, and $\mathbf{L}$ a matrix whose columns are the corresponding unitary orthogonal eigenvectors, $\mathbf{v}_i$. Then, (16) becomes

$$\mathbf{c}_\xi = b\,\mathbf{D}\,\mathbf{c}_{\xi-1} + c\,\mathbf{D}\,\mathbf{c}_{\xi-2}, \tag{17}$$

where $\mathbf{c}_\xi = \mathbf{L}^{-1}\mathbf{r}_\xi$. The decoupled difference equation (17) can be analyzed in the Z-plane domain, resulting in the following equation

$$\mathbf{I_{N\times 1}} - b\,\mathbf{D}\,\mathbf{z}^{-1} - c\,\mathbf{D}\,\mathbf{z}^{-2} = 0, \tag{18}$$

where $\mathbf{z} = [z_1, z_2, ..., z_N]^T$. Solving the decoupled quadratic equations (18) provides the poles of the vibration modes,

$$z_i^{1,2} = \frac{b\lambda_i}{2} \pm \frac{1}{2}\sqrt{b^2\lambda_i^2 + 4c\lambda_i}, \tag{19}$$

Depending on the sign of the discriminant, $\Delta_i = b^2\lambda_i^2 + 4c\lambda_i$, the resulting orthogonal mode can be underdamped ($\Delta < 0$), critical damped ($\Delta = 0$) or overdamped ($\Delta > 0$).

The largest pole (in magnitude) in a critical damped or slightly underdamped state determines the fastest speed, and its mode governs the snake dynamics towards the steady state. In order to ensure system stability, all poles must be located inside the unitary circle. Furthermore, all underdamped poles are located in the complex plane on a circle of radius $r_0 = -c/b = (2+\gamma)^{-1}$ centered at point $(r_0, 0)$ [2]. This means that in a slightly underdamped state,

- this state is reached when $-4c/b^2 \geq \lambda_{max}$, or equivalently for the following damping-mass ratio

$$\gamma_o = 2\lambda_{max}^{-1}\left(1 - \lambda_{max} + \sqrt{1 - \lambda_{max}}\right), \tag{20}$$

- the snake gets its fastest speed, and the slowest mode is assured to be less than twice the radius r_0,

$$|z_o| \leq (1 + \gamma_o/2)^{-1}. \tag{21}$$

Finally, the largest eigenvalue λ_{max} of matrix $\mathbf{H}$ depends on the stiffness parameters and mainly on N, the length of the segment between two attached nodes. An approximate rule of thumb is $\lambda_{max} = (1 - \rho N^{-1})$, where ρ is a correction term that depends on the stiffness properties of the snake.

[2] such a circumference is defined by $(x, \pm\sqrt{(x - r_0)^2 - r_0^2})$.

2.4. Non-uniformly spaced case

When N_k in (6) is non-uniformly spaced, the results from the previous sections are still valid after some reasoning. The frequency-domain eigenvectors $\mathbf{v}_i$ have a spatial-domain counterpart, $\mathbf{c}_i$, by inverse Fourier transform. Eigenvectors $\mathbf{c}_i$ are the vibration modes of the snake, and, similar to the vibration modes of a string, each segment interact with the rest by transmitting its vibration modes. In case of uniformly-spaced positions, this interaction takes place harmonically and lossless.

In case of non-uniformly spaced positions, the modes of one segment may not "propagate" harmonically if the adjacent segments have different segment lengths. In general the slowest mode of one segment may affect adjacent segments if that mode is slower than those of the adjacent segments, and if that mode is allowed to propagate. Currently, we are addressing this problem, and although conclusive results have not been achieved yet, we have seen empirically that the interaction between adjacent segments is depreciable in case of the larger ones. In case of the shortest ones (and fastest) the evolution is affected by the long segments, and the mean value of each segment speed is a fair approximation of the dynamics of the short segment.

3. SIMULATION RESULTS

In order to validate the results obtained from the analysis, a simulated segmentation problem with a closed snake was conducted. The attracted nodes were attached to certain values obtained randomly from a uniform distribution in [-1,1], this simulating the segmentation process, and the spacing between consecutive attracted nodes was randomly computed from a uniform distribution of mean value 8.

The graphical results are shown in Figures 2 and 3. Since the two spatial coordinates are independent, the results are shown only for one of them, the x-coordinate.

Regarding the final situation, top part of Fig. 2 shows the snake steady state dependence on the $H(\omega)$ filter and bottom part of this figure contains the different $G_\xi(\omega)$ filter for each case. Note that the $M + C$ value has a influence on the bandwidth of the final filter and the resulting interpolated signal.

With respect to the speed of convergence toward the final situation, Fig. 3 shows the evolution depending on the value of the damping-mass ratio γ. Three different values of γ were used, each one setting the snake in a different mode: underdamping, critical damping, and over damping node evolution.

The critical damping mode is the fastest and this mode corresponds to the situation in which the largest eigenvalue has its minimum absolute values, producing the final state curve in less iterations. Variations from this value give rise to slower convergence.

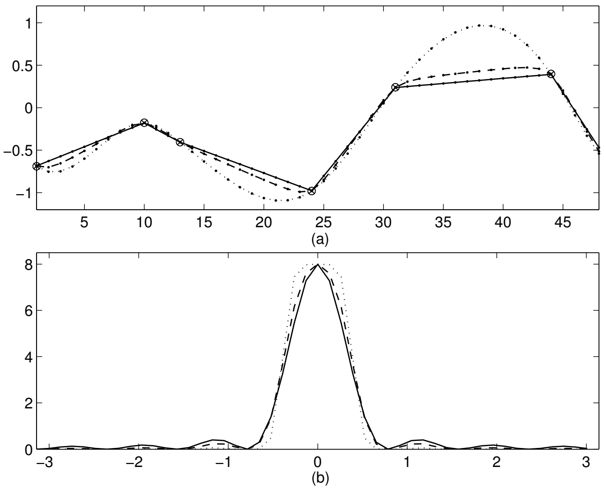

Fig. 2. Simulation results for finite difference snakes with $\alpha = 0$, $\beta = 1$ (dotted line), $\alpha = 0.5$, $\beta = 0.5$ (dashed line) and $\alpha = 1$, $\beta = 0$ (solid line). (a) Different final contours for nodes x-coordinate (b) equivalent snake spectrum $G_\xi(\omega)$.

4. CONCLUSIONS

The frequency-based formulation of active contours proposed in [5] reveals a new perspective to study and design suitable snakes. From the frequency domain several analysis can be made. In this paper, an analysis of the convergence of active contours is presented. The conclusions of the theoretical analysis are that the final solution achieved depends on the stiffness properties, $\eta = M + C$, and the $H(\omega)$ filter. Other conclusion is that the speed of the snake towards the steady state does depend on the damping-mass ratio $\gamma = M/C$.

The frequency-based analysis opens the possibility, when segmenting images, of designing the interpolation frequency kernel, apart from the original stiffness formulation, in order to achieve a specific final contour characteristics. This paper gives some hints for setting the snake parameters M and C (for a given $H(\omega)$ filter) to obtain a desired convergence towards the steady state. This goal along with the theoretical multidimensional extension cope our research work.

5. REFERENCES

[1] M. Kass, A. Witkin, and D. Terzopoulos, "Snakes: Active contour models," *Int. J of Computer Vision*, vol. 1, pp. 321–331, 1988.

[2] V. Caselles, R. Kimmel, and G. Sapiro, "Geodesic active contours," in *ICCV*, 1995, pp. 694–699.

[3] L. Weruaga, J. Morales, L. Nuñez, and R. Verdú, "Estimating volumetric motion in juman thorax with parametric matching constraints," *IEEE Trans. on Medical Imaging*, vol. 22, no. 6, pp. 766–772, June 2003.

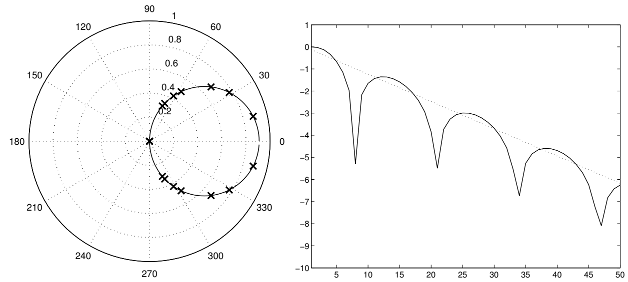

(a) Poles $\gamma = 0.2$. (b) Under damped mode.

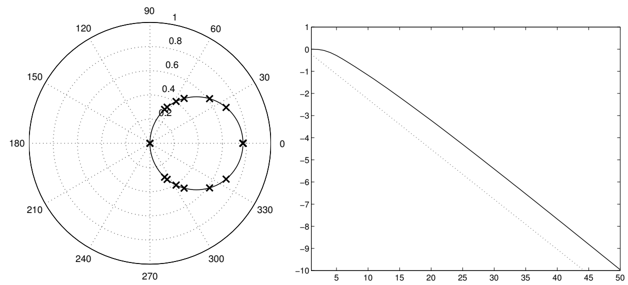

(c) Poles $\gamma = 0.5995$ (d) Critical damped mode.

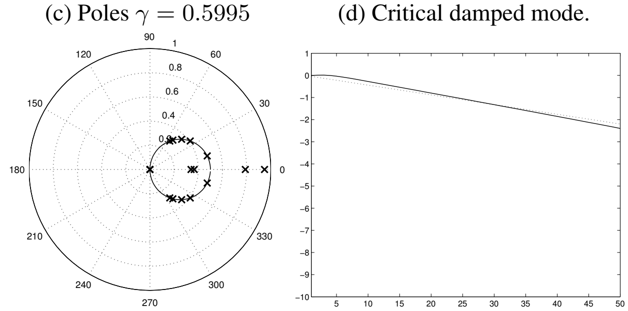

(e) Poles $\gamma = 2$. (f) Over damped mode.

Fig. 3. (a),(c) and (e) show pole location varying γ and keeping constant M. (b), (d) and (f) show the time evolution $\log(\text{abs}((x - x_{end})/(x_{ini} - x_{end}))$ for a point x of the snake.

[4] R. Verdú, J. Morales, R. Berenguer, and L. Weruaga, "Active contours for heart motion-compensated reconstruction in computed tomography," *14th Int. Conf. on DSP*, July 2002.

[5] L. Weruaga, R. Verdú, and J. Morales, "Frequency-based formulation of active deformable models," *IEEE Trans. Pattern Anal. & Mach. Intell*, accepted for publication.

[6] J. Liang, T. McInerney, and D. Terzopoulos, "United snakes," *Proc. 7th IEEE Int. Conf. on Computer Vision*, pp. 933–940, 1999.